1   **Title:** Sensorimotor expectations bias motor resonance during observation of object lifting: The causal

2   role of pSTS

3   **Abbreviated title:** Motor resonance depends on object weight expectations

4

5   Guy Rens[1,2]*, Vonne van Polanen[1,2], Alessandro Botta[3], Mareike A. Gann[1,2], Jean-Jacques Orban de

6   Xivry[1,2], Marco Davare[2,4]

7

8   [1]Movement Control and Neuroplasticity Research Group, Department of Movement Sciences,

9   Biomedical Sciences group, KU Leuven, 3001 Leuven, Belgium

10 [2]KU Leuven, Leuven Brain Institute, 3001 Leuven, Belgium

11 [3]Department of Experimental Medicine, Section of Human Physiology, University of Genoa, 16132

12 Genoa, Italy

13 [4]Department of Clinical Sciences, College of Health and Life Sciences, Brunel University London, UB8 3PN

14 Uxbridge, United Kingdom

15

16 ***Corresponding Author:**
17 Guy Rens
18 Department of Movement Sciences
19 KU Leuven
20 Tervuursevest 101,
21 3001 Leuven, Belgium
22 Guy.Rens@kuleuven.be
23
24 **Amount of pages:** 32

25 **Amount of figures:** 7

26 **Amount of tables:** 1

27 **Amount of words in abstract:** 201

28 **Amount of words in introduction:** 649

29 **Amount of words in discussion:** 1494

Abstract

Transcranial magnetic stimulation (TMS) studies have highlighted that corticospinal excitability (CSE) is increased during observation of object lifting, an effect termed as 'motor resonance'. This facilitation is driven by parameters indicative of object weight, such as object size or observed movement kinematics. Here, we investigated how motor resonance is altered when the observer's weight expectations, based on visual information, do not match the actual object weight as revealed by the observed movement kinematics. Our results highlight that motor resonance is not robustly driven by object weight but easily masked by a suppressive 'expectation monitoring mechanism' when weight expectations can be incorrect. Subsequently, we investigated whether this expectation monitoring mechanism was driven by higher-order cortical areas. For this, we induced 'virtual lesions' to either the posterior superior temporal sulcus (pSTS) or dorsolateral prefrontal cortex (DLPFC) prior to having participants perform the task. Importantly, virtual lesion of pSTS eradicated the expectation monitoring mechanism and restored object-weight driven motor resonance. In addition, DLPFC virtual lesion eradicated any modulation of motor resonance. This indicates that motor resonance is heavily mediated by top-down inputs from both pSTS and DLPFC. Altogether, these findings shed new light on the theorized cortical network driving CSE modulation during action observation.

Significance Statement

Observation of object lifting activates the observer's motor system in a weight-specific fashion: Corticospinal excitability is larger when observing lifts of heavy objects compared to light ones. Interestingly, here we demonstrate that this weight-driven modulation of corticospinal excitability is easily suppressed by the observer's expectations about object weight and that this suppression is mediated by the posterior superior temporal sulcus. Thus, our findings show that modulation of corticospinal excitability during observed object lifting is not robust but easily altered by top-down cognitive processes. Finally, our results also indicate how cortical inputs, originating remotely from motor pathways and processing action observation, overlap with bottom-up motor resonance effects.

Introduction

Over two decades ago, Fadiga et al. (1995) demonstrated for the first time the involvement of the human motor system in action observation: By applying single pulse transcranial magnetic stimulation (TMS) over the primary motor cortex (M1), they revealed that corticospinal excitability (CSE) was similarly modulated during the observation and execution of the same action. In line with the mirror neuron theory, they argued that the motor system could be involved in action understanding by bottom-up mapping ('mirroring') observed actions onto the cortical areas that are involved in their execution (for a review see: Rizzolatti et al., 2014). Consequently, action observation-driven modulation of CSE has been termed 'motor resonance'.

Recently, TMS studies in humans substantiated that motor resonance reflects parameters within the observed action. For example, Alaerts et al. (2010a, 2010b) demonstrated that motor resonance during observed object lifting is modulated by parameters indicative of object weight, such as intrinsic object properties (e.g. size), muscle contractions and movement kinematics. Specifically, CSE is facilitated when observing lifts of heavy compared to light objects. Interestingly, in a later study Alaerts et al. (2012) demonstrated that CSE is already modulated by weight during the reaching phase, suggesting a predictive mechanism underlying motor resonance as well.

However, it is important to note that these motor resonance effects do not seem to be robust. For instance, Buckingham et al. (2014) demonstrated, using the size-weight illusion, that modulation of CSE is driven by object size when observing skilled but not erroneous lifts. In addition, Senot et al. (2011) demonstrated that motor resonance based on object weight is eradicated when two objects with identical appearance but different weights are labelled the same. Lastly, Tidoni et al. (2013) demonstrated that motor resonance is altered by the intentions conveyed by the observed person as well. That is, when the actor pretended to lift a light object as if it was heavy (i.e. 'deceptive lift'), motor resonance was significantly facilitated compared to when the actor lifted the light object 'truthfully'. Although the above studies experimentally manipulated the information participants perceived, they could not investigate whether the participants' expectations changed and to which extent this altered CSE modulation.

In the present study, we wanted to probe whether the observer's expectations alter motor resonance by changing the experimental context. We asked participants to perform an object lifting task in turns with an actor. One group performed the task using objects with congruent only size-weight relationship (i.e. big-heavy or small-light objects) whereas the other group lifted objects with both congruent and incongruent properties (i.e. big-heavy, small-light and big-light, small-heavy objects).

93   Based on Alaerts et al. (2010b, 2012) findings, we hypothesized that motor resonance would be driven

94   by (i) the intrinsic object properties (i.e. size) before the observed object lift-off and (ii) the movement

95   kinematics (i.e. actual object weight) during observed lifting. However, our results revealed that, for the

96   group lifting objects with both congruent and incongruent size-weight relationships, motor resonance

97   was suppressed by an 'expectation monitoring mechanism' caused by the presence of incongruent

98   objects.

99   We carried out a second experiment to investigate whether motor resonance was suppressed by

100   top-down inputs to the motor system. We asked another group of participants to perform the same task

101   after receiving a virtual lesion of either the posterior superior temporal sulcus (pSTS) or dorsolateral

102   prefrontal cortex (DLPFC). We opted for these areas considering their involvement in understanding

103   intentions and motor goals [DLPFC: Miller and Cohen, (2001), Kilner (2012); pSTS: Nelissen et al. (2011)]

104   as well as recognizing action correctness [DLPFC: Pazzaglia et al. (2008); pSTS: Pelphrey et al. (2004)].

105   Because pSTS is reciprocally connected with the anterior intraparietal cortex (AIP) (Nelissen et al., 2011)

106   and DLPFC with the ventral premotor cortex (PMv) (Badre and D'Esposito, 2009), which are considered

107   key nodes for driving motor resonance (Rizzolatti et al., 2014), we hypothesized that virtual lesion of

108   either region would release the 'suppression' and restore weight-driven motor resonance.

109

110   **Methods**

111   Participants

112   68 participants were recruited from the student body of KU Leuven (Belgium) and divided into four

113   groups. 9 individuals were excluded prior to participation based on screening for TMS (Rossi et al., 2011)

114   and/or MRI safety (checklist of local hospital: UZ Leuven). For experiment 1, 18 individuals (12 females;

115   mean age ± SEM = 23.78 ± 0.12 years) were assigned to the control group and 17 (11 females; mean age

116   ± SEM = 24.63 ± 0.14 years) to the baseline group. For the second experiment, 24 individuals were

117   separated into two groups. Prior to performing the experimental task, 12 participants received virtual

118   lesioning of DLPFC (5 females; mean age ± SEM = 24.04 ± 0.23 years) and the other 12 received virtual

119   lesioning of pSTS (9 females; mean age ± SEM = 22.54 ± 0.18 years). The Edinburgh Handedness

120   Questionnaire (Oldfield, 1971) revealed that all participants were strongly right-handed (> 90). All

121   participants had normal or corrected-to-normal vision, were free of neurological disorders and had no

122   motor impairments of the right upper limb. Participants gave written informed consent and were

123   financially compensated for their time. The protocol was in accordance with the Declaration of Helsinki

124   and was approved by the local ethical committee of KU Leuven, Belgium (Project s60072).
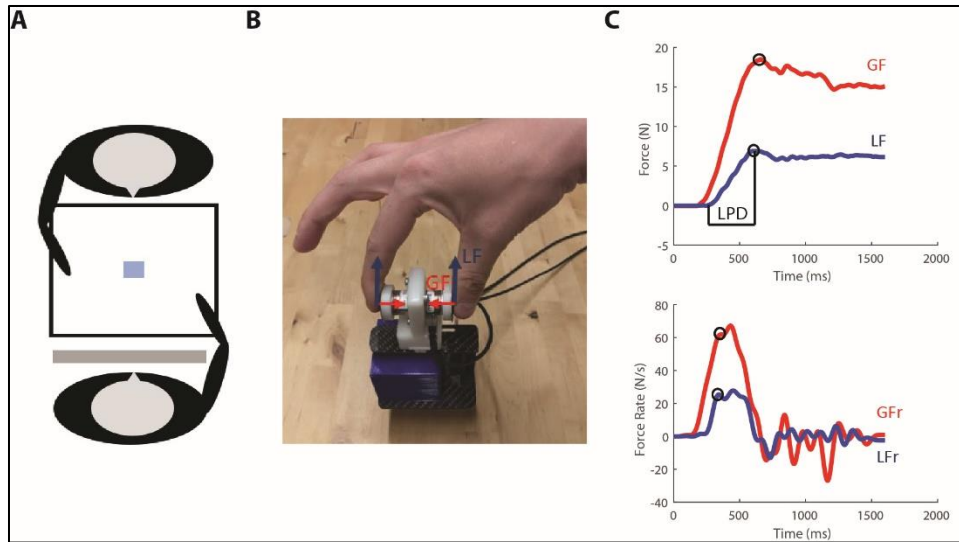
Figure 1. Experimental set-up. **A.** Representation of the experimental set-up: the participant and actor were seated opposite to each other in front of a table on which the manipulandum was positioned. A switchable screen was placed in front of the participant's face. **B.** Photo of the grip-lift manipulandum used in the experiment. Load force (LF: blue) and grip force (GF: red) vectors are indicated. **C.** GF and LF typical traces (upper) and their derivatives (lower) for a skilled lift. Circles denote first peak values used as parameters. Loading phase duration (LPD) was defined as the delay between object contact (GF > 0.20 N) and object lift off (LF > 0.98*object weight).

Experimental set-up

125

126 *Experimental task.* Subject and actor were comfortably seated opposite to each other in front of a table

127 (for the experimental set-up see: figure 1A). Participants were required to grasp and lift the

128 manipulandum (see: 'acquisition of force data') that was placed in front of them in turns with the actor.

129 As such, one trial consisted of one lifting action performed by either the actor ('actor trial') or the

130 participant ('participant trial'). Prior to the start of the task, participants received two practice trials on

131 the objects with a congruent size-weight relationship ('congruent objects') but not on those with an

132 incongruent relationship ('incongruent objects'; for an explanation see: 'acquisition of force data').

133 Participants also received the following instructions beforehand: (1) Lift the manipulandum to a height of

134 approximately 5 cm at a smooth pace that is natural to you. (2) Only place thumb and index finger on the

135 graspable surfaces (precision grip). (3) The cube in your trial always matches the cube in the actor's

136 preceding trial both in size and weight. As such, participants always lifted the exact same cube as the

137 actor did in the preceding trial and could rely on lift observation to estimate object weight for their own

138 trials (Rens and Davare, 2019). Finally, both participants and actor were asked to place their hand on a

139 predetermined location on their side of the table to ensure consistent reaching throughout the

140 experiment. Reaching distance was approximately 25 cm and required participant and actor to use their

5

141   entire right upper limb to reach for the manipulandum. Lastly, participants were not informed about the

142   incongruent objects prior to the start of the experiment.

143   For experiment 1 (control and baseline groups), each trial performed by the actor or the

144   participant was initiated with a neutral sound cue ('start cue'). For experiment 2 (DLPFC and pSTS

145   groups), we removed the start cue as we applied TMS during participant trials as well (see the 'TMS

146   procedure and EMG recording' section for the stimulation conditions; see the 'Experimental groups'

147   paragraph below for the inter-group differences). Accordingly, participants in experiment 2 were

148   instructed to consider the TMS pulse as the start cue and only initiate their movement after TMS was

149   applied. For all groups, trials lasted 4 s to ensure that participants and actor had enough time to reach,

150   grasp and lift the manipulandum smoothly at a natural pace. Inter-trial interval was approximately 5 s

151   during which the cuboid in the manipulandum could be changed. A transparent switchable screen (Magic

152   Glass), placed in front of the participant's face, became transparent at trial onset and turned back to

153   opaque at the end of the trial. The screen remained opaque during the inter-trial interval to ensure

154   participants had no vision on the cube switching. The actor always performed the act of changing the

155   cuboid before executing his trials (even if the same cube would be used twice in a row). This was done to

156   ensure that participants could not rely on sound cues to predict cube weight in the actor's upcoming

157   trial. Switching actions were never performed before participant trials as they were explained that their

158   cube would always match that of the actor.

159   *Experimental procedure.* All participants performed the object lifting task in a single session

160   ('experimental session'). Moreover, participants of experiment 2 underwent prior MRI scanning (session

161   duration: 30 min) on a different day. At the start of the experimental session (start of scanning session

162   for the participants of experiment 2), participants gave written informed consent and were prepared for

163   TMS stimulations as described below. Afterwards participants performed the experimental task (for the

164   amount of trials per group see: table 1). For the baseline group, the total amount of trials was divided

165   over four experimental blocks. Participants in the control, DLPFC and pSTS groups performed two

166   experimental blocks. The proportion of trials on each cube was equal in all blocks and participants

167   received a short break between blocks. Lastly, the experimental session lasted 60 minutes for the control

168   group and 90 minutes for the baseline, DLPFC and pSTS groups. Differences in session duration between

169   the groups resulted from differences in TMS preparation and the amount of trials per group.

170   *Experimental groups.* In experiment 1, we wanted to investigate whether the presence of

171   incongruent objects alters motor resonance. For this, we divided participants into two groups, which

172   were the control and baseline group. Participants in the control group were only exposed to the

173   congruent objects. In contrast, participants in the baseline group lifted both the congruent and

174   incongruent objects during the task. Importantly, as we wanted the baseline group to anticipate that the

175   object's size and weight were congruent, we decided to use unequal proportions of congruent and

176   incongruent trials (33 % of trials were incongruent; see discussion for limitations) (table 1).

Table 1. Amount of trials per observational condition for each of the four experimental groups

		Congruent lifts (per person per weight)			Incongruent lifts (per person per weight)			Total amount of trials	Ratio of incongruent trials
	TMS applied	none	observed contact	after observed lift-off	none	observed contact	after observed lift-off		
Group	Control	6	18	18	/	/	/	168	/
	Baseline	16	16	16	/	12	12	288	33 %
	DLPFC	12	/	24	/	/	12	192	25 %
	pSTS	12	/	24	/	/	12	192	25 %

Table 1. Distribution of trials per observational condition. In order to reach the full amount of trials, each amount has to be two times multiplied by two. Once for the participants (as trials only reflect observed trials) and once for the two weights (heavy and light) that have been used. For example: participants in the control experiment only performed lifts on the congruent cubes. During observation (actor trials), TMS was not applied in 6 trials, applied at observed object contact (18 trials) or after observed lift-off (18 trials). Accordingly, participants observed 42 lifts (all timings combined) for one congruent cube. Considering that we used two congruent cubes, participants observed 82 trials in total. Moreover, as participants performed the task in alternation with the actor, they also performed 82 trials. As a result, during the experimental session of a participant in the control group, 168 trials in total were performed.

177   In experiment 2, we wanted to investigate how pSTS and DLPFC are causally involved in

178   mediating the suppressive mechanism revealed in experiment 1. Participants performed the same task

179   as the baseline group of experiment 1 after receiving a virtual lesion over either pSTS or DLPFC.

180   Compared to the baseline group, participants performed approximately 100 trials less due to time

181   constraints related to the procedure used to induce the virtual lesion (Huang et al., 2005). We also

182   reduced the proportion of incongruent trials (25 % of trials were incongruent; table 1) to ensure they

183   appeared at a reduced absolute frequency in order to have participants maintain their size-weight

184   expectations. Arguably, the different proportions of erroneous trials should not affect CSE modulation

185   differently: Pezzetta et al. (2018) demonstrated, using electro-encephalography (EEG), that errors rather

186   than their probability elicit typical error-related cortical activation. Moreover, if the suppressive

187   mechanism would be rather driven by the relative frequency of the error occurrence than by the error

188   itself, then the effects of the suppressive mechanism on CSE modulation should be enhanced rather than

189   decreased with a lower proportion of incongruent trials.

190

191

192   Acquisition of force data

193   A grip-lift manipulandum consisting of two 3D force-torque sensors was attached to a custom-

194   made carbon fibre basket in which different objects could be placed (for an image of the manipulandum

195   see: figure 1B). The total weight of the manipulandum was 1.2 N. The graspable surface (17 mm

196   diameter and 45 mm apart) of the force sensors was covered with fine sandpaper (P600) to increase

197   friction. For the present experiment, we used four 3D-printed objects. The large objects (cuboids) were

198   5x5x10 cm in size whereas the two small ones (cubes) measured 5x5x5 cm. Two of the objects, one small

199   and one large, were filled with lead particles so each of them weighted 0.3 N. The other two were filled

200   with lead particles until each of them weighted 5 N. Combined with the weight of the manipulandum,

201   the light and heavy objects weighted 1.5 and 6.3 N respectively. Importantly, using these four objects,

202   we had a two by two design with size (small or big) and weight (light or heavy) as factors. In addition, this

203   design allowed us to have two objects that were 'congruent' in size and weight (large objects are

204   expected to be heavier than smaller ones of the same material) and two 'incongruent' objects for which

205   this size-weight relationship was inversed (Baugh et al., 2012). To exclude any visual cues indicating

206   potential differences between the same-sized objects, they were hidden under the same paper covers. In

207   the present study, we used two ATI Nano17 F/T sensors (ATI Industrial Automation, USA). Both F/T

208   sensors were connected to the same NI-USB 6221 OEM board (National Instruments, USA) which was

209   connected to a personal computer. Force data was acquired at 1000 Hz using a custom-written Labview

210   script (National Instruments, USA). Lastly, one of the authors G. Rens served as the actor in both

211   experiment 1 and 2.

212

213   TMS procedure and EMG recording

214   *General procedure*. For all groups, electromyography (EMG) recordings were performed using Ag-AgCl

215   electrodes which were placed in a typical belly-tendon montage over the right first dorsal interosseous

216   muscle (FDI). A ground electrode was placed over the processus styloideus ulnae. Electrodes were

217   connected to a NL824 AC pre-amplifier (Digitimer, USA) and a NL820A isolation amplifier (Digitimer, USA)

218   which in turn was connected to a micro140-3 CED (Cambridge Electronic Design Limited, England). EMG

219   recordings were amplified with a gain of 1000 Hz, high-pass filtered with a frequency of 3 Hz, sampled at

220   3000 Hz using Signal software (Cambridge Electronic Design Limited, England) and stored for offline

221   analysis. For TMS stimulation, we used a DuoMAG 70BF coil connected to a DuoMAG XT-100 system

222   (DEYMED Diagnostic, Czech Republic). For M1 stimulation, the coil was tangentially placed over the

223   optimal position of the head (hotspot) to induce a posterior-anterior current flow and to elicit motor

224   evoked potentials (MEPs) in right FDI. The hotspot was marked on the scalp of each participant.

225   Stimulation intensity (1 mV threshold) for each participant was defined as the lowest stimulation

226   intensity that produced MEPs greater than 1 mV in at least four out of eight consecutive trials when

227   stimulating at the predetermined hotspot. Lastly, the control group and baseline group received 12

228   stimulations at the 1 mV threshold before and after the experiment to have a baseline measure of

229   resting CSE. Moreover, for the baseline group, we also recorded a baseline measure of resting CSE

230   halfway through the experiment (i.e. when participants had performed half of the experimental blocks)

231   as their experimental session lasted 30 min longer.

232   *Stimulation during the experimental task*. For the control and baseline group, TMS was applied

233   during the actor trials at two different timings: at object contact and during the lifting phase (see 'Data

234   processing' for their definitions). Participants did not receive stimulations during their trials (i.e.

235   participant trials). For the DLPFC and pSTS groups, TMS was applied during both the actor and participant

236   trials. During observation we only applied TMS during the observed lifting phase, and not at observed

237   contact for two reasons: (1) The results from experiment 1 indicated that CSE was primarily modulated

238   during observed lifting and (2) because of the time constraints related to the duration of the after-effects

239   caused by cTBS (Huang et al., 2005), which are limited to about an hour. During participant trials, TMS

240   was applied 400 ± 100 ms (jitter) after object presentation. As participants were instructed to only start

241   lifting after receiving the stimulation, it was applied during movement planning and not execution. We

242   did not stimulate the control and baseline groups during lift planning because initially we were only

243   interested in motor resonance. We did include these stimulations in experiment 2, because we wanted

244   to investigate the effect of a virtual lesion of DLPFC or pSTS on this inhibition during motor planning.

245   Finally, in experiment 1 (control and baseline groups) we did not use neuro-navigation but relied on the

246   hotspot mark on the scalp to stimulate M1 during the experiment. In contrast, for experiment 2 (DPLFC

247   and pSTS groups) we used neuro-navigation for applying cTBS but also for maintaining the same coil

248   positioning and orientation during the experiment. Accordingly, for experiment 2, the hotspot was

249   determined using the same procedures as in experiment 1, although the M1 stimulations during the

250   experiment were neuro-navigated. However, this should not have affected the validity of our between-

251   group differences (for example see: Jung et al., 2010).

252   *Additional procedures for experiment 2*. After defining the 1 mV threshold, we defined

253   the active motor threshold (aMT) as the lowest stimulation intensity that produced MEPs that were

254   clearly distinguishable from background EMG during a voluntary contraction of about 20 % of their

255   maximum using visual feedback. Before the experimental task, participants received cTBS over either

256　　DLPFC or pSTS. cTBS consisted of bursts of 3 pulses at 50 Hz, repeated with a frequency of 5 Hz and at an

257　　intensity of 80 % of the aMT for 40 s (600 pulses in total). It has been considered that this type of

258　　repetitive stimulation disrupts activity within the stimulation region for a period up to 60 minutes (Huang

259　　et al., 2005). Consequently, it has often been termed a 'virtual lesion'. In experiment 2, we also collected

260　　resting CSE before cTBS. As such, we recorded three resting CSE measurements, i.e. pre-cTBS, pre-task (5

261　　minutes after cTBS ended and just before the start of the experimental task) and post-task. To ensure

262　　that cTBS was applied on the desired stimulation area, a high-resolution structural T1-weighted

263　　anatomical image of each participant was acquired with a magnetization-prepared rapid-acquisition

264　　gradient-echo (MPRAGE) sequence (Philips Ingenia 3.0T CX, repetition time/echo time = 9.72/4.60 ms;

265　　voxel size = 1.00 X 1.00 X 1.00 mm^3; field of view = 256 X 256 X 192 mm^3; 192 coronal slices) which was

266　　co-registered during the experiment with the fiducial landmarks using a Brainsight TMS neuronavigation

267　　system (Rogue Research, Canada).
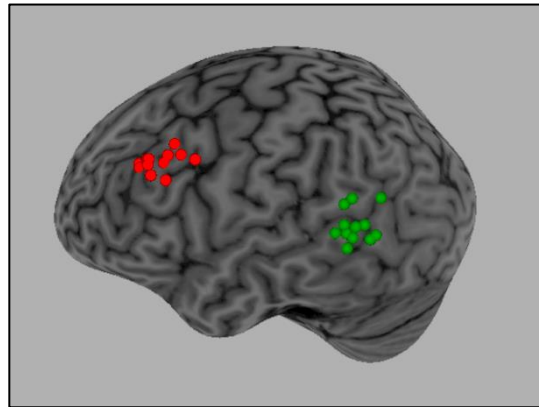
Figure 2. Stimulation sites. Anatomical locations where cTBS was applied for each individual subject of the DLPFC (red) and pSTS (green) groups.

268　　　　DLPFC was anatomically identified following Mylius et al. (2013). Briefly, we identified the

269　　superior and inferior frontal sulci as the superior and inferior borders of the middle frontal gyrus (MFG).

270　　The posterior border was defined as the precentral sulcus and the frontal one as the anterior

271　　termination of the olfactory sulcus in the coronal plane. Lastly, the MFG was divided equally into three

272　　parts and the separating line between the anterior and middle thirds was defined as the DLPFC (for full

273　　details see: Mylius et al., 2013). We always defined DLPFC within the middle frontal sulcus (MFS). This

274　　allowed us to consistently target the MFS using the same coil orientation across participants. Coil

275　　orientation was perpendicular to the MFS with the handle pointing downwards. pSTS was anatomically

276　　defined following Cattaneo et al. (2010) and Arfeller et al. (2013) as the middle between the caudal and

277   rostral ends of the ascending branch of STS, just below the intraparietal sulcus. Coil orientation was

278   perpendicular to pSTS with the handle pointing downwards. The means ± SEM of Talaraich coordinates

279   for these sites were as follows: left DLPFC: X = -38.14 ± 0.93, Y = 23.53 ± 1.64, Z = 32.29 ± 0.80; left pSTS:

280   X = -54.03 ± 1.09, Y = -49.86 ± 1.32, Z = 9.35 ± 1.22 as estimated on the cortical surface (For stimulation

281   locations see: figure 2) which are in line with previous studies [left DLPFC: X = -42.17 ± 5.07, Y = -33.73 ±

282   5.73, Z = 32.36 ± 6.17 Mylius et al. (2013); left pSTS: X = -51.6 ± 3.6, Y = -43.2 ± 7.1, Z = 7.1 ± 6.4 Arfeller

283   et al. (2013)]

284

285   Data processing

286   *Force data.* Data collected with the F/T sensors were low-pass filtered with a fifth-order Butterworth

287   filter (forces cut-off frequency: 30 Hz, force rates cut-off frequency: 15 Hz). A custom script was written

288   in MATLAB to compute the following variables: (1) Grip (GF) and load (LF) forces, which were defined as

289   the exerted force perpendicular and tangential to the normal force, respectively (figure 1B). GF and LF

290   were computed as the sum of the respective force components exerted on both sensors. Additionally,

291   grip and load force rates (GFr and LFr) were computed by taking the first derivative of GF and LF

292   respectively. We report not GF and LF but their rates (figure 1C) as it has been demonstrated that force

293   rate parameters are a reliable indicator of predictive force scaling (Johansson and Westling, 1988b;

294   Gordon et al., 1991). For analyses purposes of the force parameters, we decided to use the first peak grip

295   and load force rate values after object contact that were at least 30 % of the maximum peak rate. This

296   threshold was used to exclude small peaks in the force rates due to noise or small bumps caused by

297   lightly contacting the F/T sensors. In addition, we decided to use the first peak force rate values as later

298   peak values might be contaminated with feedback mechanisms and not reflect predictive force planning

299   (Castiello, 2005; Rens and Davare, 2019). Accordingly, using the peak force rates enabled us to

300   investigate whether participants scaled their fingertips forces differently for the incongruent and

301   congruent objects. Besides peak force rates, we also report the loading phase duration (LPD) which was

302   defined as the latency between object contact and lift off. Object contact and lift-off were defined as the

303   time points when GF exceeded 0.2 N and LF exceed 0.98 x object weight (figure 1C), respectively. We

304   included LPD as it is considered an estimator of the lifting speed [e.g. the shorter the LPD the faster the

305   object will be lifted: Johansson and Westling (1988a)], which is a movement parameter used by

306   participants to estimate object weight (Hamilton et al., 2007). Moreover, we could also use this

307   parameter to investigate the participants' lifting performance. Lastly, both force rate parameters and

308   LPD were z-score normalized. For the participants, z-score normalization was done for each participant

309   separately. For the actor, z-score normalization was also done for each 'participant' separately. That is,

310   the actor's lifting performance in one session (as observed by one participant) was z-score normalized

311   against the data of only that session. We decided to normalize our data based on the assumption that

312   the actor's lifting speed might vary and this might affect the participants' lifting speed as well.

313   Accordingly, z-score normalization would enable us compare between-group differences (Rens and

314   Davare, 2019).

315   *EMG data.* From the EMG recordings, we extracted the peak-to-peak amplitudes of the MEP

316   using a custom-written MATLAB script. All EMG recordings were visually inspected for background noise

317   related to muscle contractions. Moreover, trials were excluded when the MEP was visibly contaminated

318   (i.e. spikes in background EMG) or when an automated analysis found that the average background EMG

319   was larger than 50 μV (root-mean-square error) in a time window of 200 ms prior to the TMS

320   stimulation. Lastly, for each participant separately we excluded outliers which we defined as values

321   exceeding the mean ± 3 SD's. For each participant, all MEPs collected during the experimental task (but

322   not resting measurements) were normalized with z-scores using their grand mean and standard

323   deviation. For experiment 2, z-scoring was done for lift observation and planning separately.

324

325   <u>Statistical analysis</u>

326   *Corticospinal excitability during rest.* To investigate within-group differences in baseline CSE, we

327   performed repeated measures analyses of variance (ANOVA$_{RM}$) for the control and the baseline group

328   separately with one within-factor RESTING STATE (control: pre- and post-task; baseline; pre-task,

329   between experimental blocks, post-task). For experiment 2, we performed a mixed ANOVA with

330   between-factor GROUP (DLPFC or pSTS) and within factor RESTING (pre-cTBS, pre-task, post-task).

331   *Within-group differences for corticospinal excitability during the experimental task.* First, to

332   investigate whether our experimental task can elicit weight-driven motor resonance effects during lift

333   observation, we performed a ANOVA$_{RM}$ on the control group only with within-factors CUBE (big heavy or

334   small light) and TIMING (observed contact or after observed lift-off). To investigate whether the

335   presence of the incongruent objects altered motor resonance, we used a general linear model (GLM; due

336   to different effect sizes) to probe potential differences between the control and baseline groups on the

337   congruent objects only. We used the between-factor GROUP (control or baseline) and within-factors

338   CUBE and TIMING. Due to our findings, we followed up on this GLM with a ANOVA$_{RM}$, only performed on

339   the baseline group with within-factors TIMING, SIZE (big or small) and WEIGHT (heavy or light).

340   After these analyses on the groups of the first experiment, we investigated the potential effects

341   of the virtual lesions of DLPFC and pSTS. For this, we performed a GLM with between-factor GROUP

342   (baseline, DLPFC or pSTS) and within-factors SIZE and WEIGHT. As we did not stimulate the DLPFC and

343   pSTS groups at observed contact, we could not include the within-factor TIMING. As we wanted to

344   further explore potential within-group effects, we followed up on the GLM with separate ANOVA$_{RM}$s for

345   the DLPFC and pSTS groups with within-factors SIZE and WEIGHT. Finally, to explore potential differences

346   between lift observation and planning for the groups of experiment 2, we performed a final GLM with

347   between-factor GROUP (DLPFC or pSTS) and within-factors ACTION (observation or planning), SIZE and

348   WEIGHT.

349   *Force parameters of the participants*. For each parameter of interest (peak GFr, peak LFr and

350   LPD), we performed a GLM on the congruent objects only with between-factor GROUP (control, baseline,

351   DLPFC or pSTS) and within-factor CUBE (big heavy or small light). We performed an additional GLM on

352   the congruent and incongruent objects combined with between-factor GROUP (baseline, DLPFC or pSTS;

353   control not included due to not using the incongruent objects) and within-factors SIZE and WEIGHT.

354   Importantly, within-factors related to the timing of the TMS stimulation are not included here as our

355   preliminary analyses indicated that it did not affect predictive force planning in the participants, i.e. we

356   did not find significance for any of the relevant pairwise comparisons. Because of these findings, we

357   decided to pool the data for TIMING and present the data as such for clarity.

358   *Force parameters of the actor*. For each parameter (peak GFr, peak LFr and LPD) we performed

359   the same analyses as described in 'Force parameters of the participants'. We did not include the within-

360   factors related to timing as the actor was blinded to the timings during the experiment.

361   Lastly, for the GLMs we used type III sum of squares, comparisons of interest exhibiting

362   statistically significant differences *(p ≤ 0.05)* were further analysed using the Holm-Bonferroni test. All

363   data presented in the text are given as mean ± standard error of the mean. All analyses were performed

364   in STATISTICA (Dell, USA).

365

366   **Results**

367   In the present study, we investigated how motor resonance is modulated during lift observation. For

368   this, participants performed an object lifting task in turns with an actor. The control group only lifted

369   objects with a congruent size-weight relationship (i.e. 'big heavy' and 'small light' objects). The baseline

370   group lifted objects with both congruent and incongruent size-weight relationships (i.e. additional 'big

371   light' and 'small heavy' objects). The subject groups participating in experiment 2 (DLPFC and pSTS

13

372   groups) used the same objects as the baseline group. Importantly, they performed the experimental task

373   after receiving a TMS induced virtual lesion over either DLPFC or pSTS. Only relevant main and

374   interaction effects are reported below.

375   <u>Stimulation intensities</u>

376   To examine differences between stimulation intensities of the different groups, we ran two GLMs to

377   investigate group differences in 1 mV thresholds (all groups) and aMT (DLPFC and pSTS groups only). All

378   values are expressed as a percentage of the maximal stimulator output. As expected, the GLM failed to

379   reveal any significant difference between groups for the 1 mV stimulation intensity (control = 61 % ±

380   2.62; baseline = 55.64 % ± 3.26; DLPFC = 57.54 % ± 3.26; pSTS = 50.46 % ± 3.00) $(F_{(3,48)}$ = 2.39 $p = 0.08, \eta^2_p$

381    $= 0.13)$ as well as for the aMT (DLPFC = 42.82 % ± 2.26; pSTS = 38.46 % ± 2.08) $(F_{(1,22)}$ = 2.01 $p = 0.17, \eta^2_p =$

382    $0.08).$ Note that the degrees of freedom of the error are lower due to missing values.

383   We informally asked participants in experiment 2 how they perceived cTBS. In the DLPFC group,

384   2 out of 12 participants described cTBS as 'uncomfortable' whereas the other ten did not report negative

385   sensations. In the pSTS group, five participants reported negative sensations: four reported the

386   sensations as 'uncomfortable' and one as 'painful'. Lastly, no one reported other physical adverse effects

387   (such as dizziness or headaches) that could potentially have been related to the single pulse or cTBS

388   stimulations.

389

390   <u>Corticospinal excitability at rest</u>

391   *Experiment 1.* For the control (pre-task = 0.89 mV ± 0.08; post-task = 1.16 mV ± 0.22) and baseline groups

392   (pre-block 1 = 0.61 mV ± 0.06; between-blocks = 0.79 mV ± 0.18; post-block 2 = 0.87 mV ± 0.17), both

393   analyses indicated that resting CSE did not change significantly over time (non-significance of TIMING;

394   *both F < 167, both p > 0.21, both η^2_p < 0.09).*

395   *Experiment 2.* Both the main effects of GROUP, TIMING as well as their interaction effect were

396   not significant *(all p > 0.16)* indicating that resting CSE did not differ between groups and did not change

397   over time (DLPFC: pre-cTBS = 1.16 mV ± 0.26, pre-task = 1.53 mV ± 0.22, post-task = 1.60 mV ± 0.44;

398   pSTS: pre-CTBS = 2.04 mV ± 0.26, pre-task = 1.60 mV ± 0.22, post-task = 2.20 mV ± 0.44).

399

400   *<u>Corticospinal excitability during the experimental task</u>*

401   First of all, we investigated, using the control group, whether our task can elicit weight driven

402   modulation of CSE during observed object lifting. As shown on figure 3, the analysis substantiated the

403   validity of our set-up: When the control group observed lifts of the big heavy object (big heavy = 0.07 ±
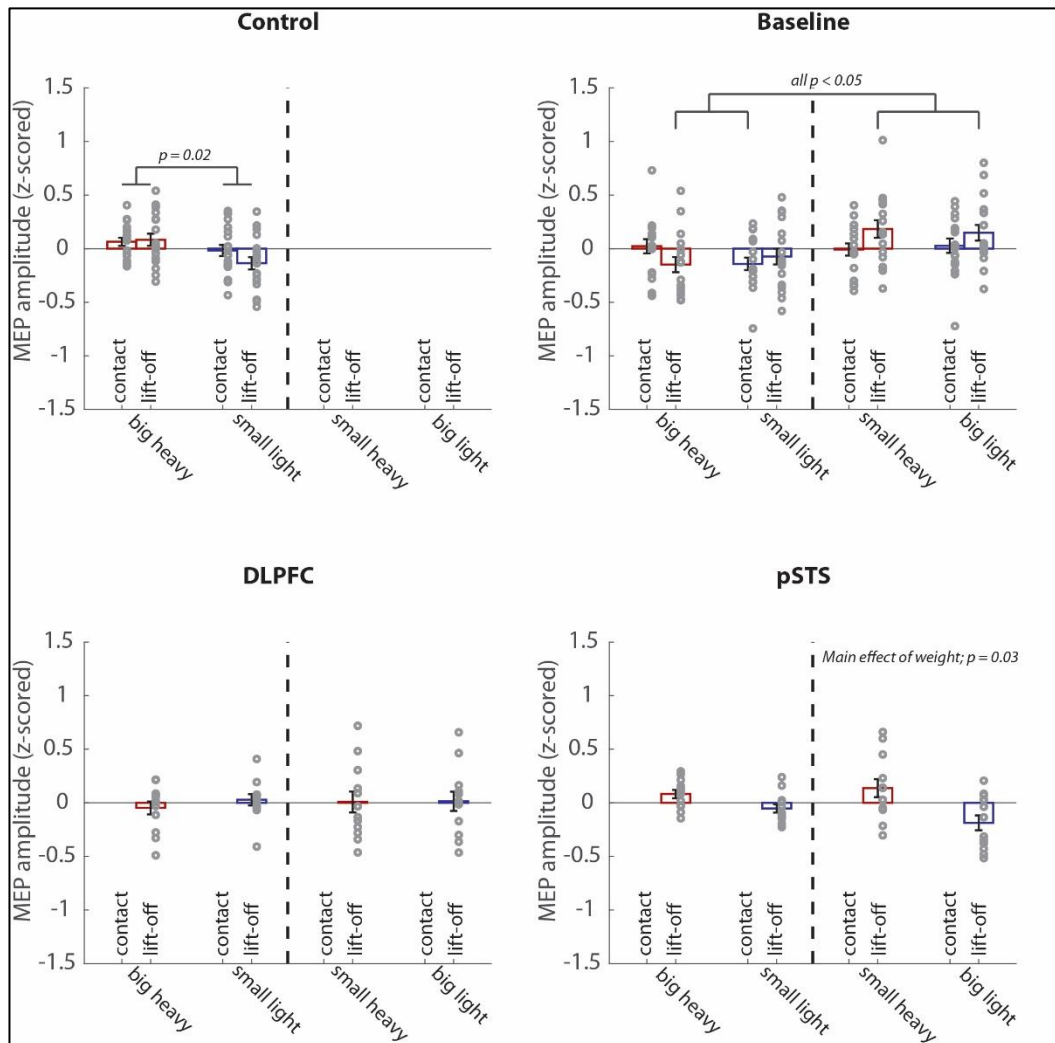
Figure 3. Modulation of corticospinal excitability during lift observation. Average MEP values (z-score) during lift observation pooled across participants for each experimental group separately. Left and right of the dashed line on each figure represent the congruent (big heavy and small light) and incongruent objects (small heavy and big light) respectively. Red and blue indicate heavy and light weights respectively. For the control and baseline groups we used two TMS timings during observation, i.e. at observed object contact and after observed lift-off. As such, of two adjacent bars, the first and second one represent MEP values at observed contact and during observed lifting respectively. For the DLPFC and pSTS groups we used only one TMS timing (object lift off). Each circle (scatter) represents the average MEP value for one participant in that specific condition. All data is presented as the mean ± SEM. Only significant intra-group differences are shown on these graphs.

404   0.03) CSE was significantly facilitated compared to when they observed lifts of the small light object

405   (small light = -0.08 ± 0.03; *p = 0.02*) *(main effect of CUBE: $F_{(1,17)} = 6.87$, p = 0.02, $\eta^2_p = 0.29$).*

406   Second, we explored whether the presence of the incongruent objects affected CSE modulation.

407   For this, we compared the control and baseline groups for only the congruent objects. In line with our

408   findings for the control group, CSE was significantly facilitated when observing lifts of the big heavy cube

409 (big heavy = 0.006 ± 0.02) compared to the small light one (small light = -0.09 ± 0.03; *p = 0.04*) *(main*

410 *effect of CUBE: $F_{(1,33)}$ = 4.34, p = 0.04, η^2_p = 0.12).* However, the main effect of GROUP *($F_{(1,33)}$ = 7.30, p =*

411 *0.01, η^2_p = 0.18)* was significant as well: When observing lifts (of the congruent objects) CSE of the

412 baseline group (congruent objects = -0.09 ± 0.02) was significantly more inhibited than that of the

413 control group (congruent objects = 0.00 ± 0.02). Considering that the group averages for CSE (MEP-

414 amplitude) are calculated using z-score normalization, these findings indicate that the presence of the

415 incongruent objects in the baseline experiment should have inhibited CSE modulation for the congruent

416 objects (due to negative z-score). In addition, this notion of the incongruent object's presence altering

417 CSE modulation might be supported by the borderline significance of the interaction effect CUBE X

418 TIMING X GROUP *($F_{(1,33)}$ = 3.71, p = 0.06, η^2_p = 0.10).*

419   To probe these potential differences between the congruent and incongruent objects for the

420 baseline group, we decided to perform a separate ANOVA_{RM} on the baseline group with within-factors

421 TIMING, SIZE and WEIGHT. Interestingly, this analysis revealed that CSE modulation in the baseline group

422 was not driven by SIZE or WEIGHT but by 'congruency'. As shown on figure 3, CSE was significantly more

423 facilitated for the small heavy object during observed lifting (mean = 0.18 ± 0.08) compared to the big

424 heavy one during observed lifting (mean = -0.15 ± 0.07; *p = 0.01*) and the small light one at observed

425 contact (mean = -0.14 ± 0.06; *p = 0.02*) *(interaction effect of WEIGHT X SIZE X TIMING: $F_{(1,16)}$ = 7.54, p =*

426 *0.01, η^2_p = 0.32).* Conversely, CSE was significantly more facilitated during observed lifting of the big light

427 object (mean = 0.15 ± 0.08), compared to the big heavy one during observed lifting *(p = 0.03)*, and the

428 small light one at observed contact *(p = 0.04)* (*SIZE X WEIGHT X TIMING*). Importantly, these findings

429 contradict our initial hypothesis: We expected that motor resonance would be driven by SIZE at

430 observed contact and afterwards by WEIGHT during observed lifting. However, our results demonstrated

431 that motor resonance effects driven by size or weight were 'masked' by a mechanism that is monitoring

432 object congruency, i.e. monitoring a potential mismatch between anticipated and actual object weight.

433   Third, we investigated the potential effects of the virtual lesions on CSE modulation during lift

434 observation. As described in 'Statistical analysis', we performed a GLM with between-factor GROUP

435 (baseline, DLPFC and pSTS groups) and within-factors SIZE and WEIGHT. As shown on figure 3, this

436 analysis revealed that for the pSTS group, CSE was significantly facilitated when observing lifts of heavy

437 objects, irrespective of their size (heavy objects = 0.11 ± 0.05) compared to lifts of the light ones (light

438 objects = -0.12 ± 0.04; *p = 0.03*) *(interaction effect of GROUP X WEIGHT: $F_{(2,38)}$ = 4.97, p = 0.01, η^2_p = 0.17).*

439 However, this weight-driven modulation of CSE during lift observation was absent for the baseline group

440 (due to the congruency effect as described above; heavy objects = 0.02 ± 0.04; light objects = 0.04 ± 0.03;

441   *p = 1.00)* but was also absent for the DLPFC group (heavy objects = -0.02 ± 0.05; light objects = 0.02 ±

442   0.04; *p = 1.00) (GROUP X WEIGHT)*. As such, these findings indicate that weight-driven modulation of CSE

443   during lift observation was restored for the pSTS group. However, these results also indicate that CSE

444   was not modulated after DLPFC was virtually lesioned.

445   To further investigate the WEIGHT effect in the pSTS group, we performed an additional GLM for

446   the control and pSTS groups combined. Indeed, if weight-driven modulation of CSE during lift

447   observation was restored by virtual lesioning of pSTS, then the pSTS group should have not differed

448   significantly from the control group with respect to the congruent objects. For this analysis, we used the

449   between-factor GROUP (control and pSTS) and within-factor CUBE (big heavy and small light) for TIMING

450   being only after observed lift-off (as we did not apply TMS at observed contact in the pSTS group).

451   Importantly, the main effect of CUBE was significant *(F$_{(1,28)}$ = 6.43, p = 0.02, η²$_p$ = 0.19)*. In line with our

452   control group findings, CSE was significantly facilitated when observing lifts of the big heavy object (big

453   heavy = 0.08 ± 0.04) compared to observing lifts of the light one (small light = -0.09 ± 0.04; *p =*

454   *0.01)*.Interestingly, this analysis did not show significance for the main effect of GROUP as well as for its

455   interaction with CUBE *(both F < 0.03, both p > 0.28, both η²$_p$ < 0.04)*. As such, these findings further

456   substantiate that in both the control and pSTS group, CSE modulation during lift observation was driven

457   by the object's actual weight (figure 3).

458   Moreover, we explored whether CSE was still modulated by object weight after virtual lesioning

459   of DLPFC using the same analysis as described above for the pSTS group (however, the groups in this

460   analysis are the control and DLPFC groups). Briefly, this analysis failed to reveal significance for any of the

461   main effects (GROUP and CUBE) as well as their interaction effect *(all F < 3.57, all p > 0.06, all η²$_p$ < 0.11)*

462   further substantiating that there is no evidence that CSE was modulated by observed object weight after

463   virtual lesioning of DLPFC. To ensure that the borderline significant interaction effect was not caused by

464   the DLPFC group, we performed a final ANOVA$_{RM}$ on the DLPFC group with one within-factor CUBE.

465   Again, this analysis failed to show significance for CUBE *(F$_{(1,11)}$ = 0.54, p = 0.48, η²$_p$ = 0.05)*. In conclusion,

466   there is no evidence that CSE was modulated during lift observation at all when DLPFC was virtually

467   lesioned.

468   To end, we investigated whether CSE was modulated differently during lift observation and

469   planning for the DLPFC and pSTS groups using a GLM with between-factor GROUP and within-factors

470   ACTION (observation or planning), SIZE and WEIGHT. Interestingly, this analysis showed that CSE was

471   significantly facilitated when observing or planning lifts of the heavy objects (heavy objects = 0.03 ± 0.02)

472   compared to of the light ones (light objects = -0.05 ± 0.02; *p = 0.02) (main effect of WEIGHT: F$_{(1,22)}$ = 6.68,*

17

473   *p = 0.02, η²$_p$ = 0.23)*. However, this WEIGHT effects was likely driven by the pSTS group as the significant

474   interaction effect GROUP X WEIGHT *(F$_{(1,22)}$ = 5.66, p = 0.03, η²$_p$ = 0.20)* revealed that WEIGHT drove CSE

475   modulation in the pSTS (heavy objects = 0.06 ± 0.02; light objects = -0.08 ± 0.03; *p = 0.01)* but not in the

476   DLPFC group (heavy objects = -0.00 ± 0.02; light objects = -0.01 ± 0.03; *p = 1.00)*. In its turn, the

477   significant difference between CSE modulation by the heavy and light objects for the pSTS group (GROUP

478   X WEIGHT) was likely driven by the triple interaction effect GROUP X ACTION X WEIGHT *(F$_{(1,22)}$ = 4.31, p =*

479   *0.05, η²$_p$ = 0.16)*. Post-hoc exploration of this significant interaction effect revealed that, for the pSTS

480   group, CSE was significantly facilitated during lift observation of the heavy objects (heavy objects = 0.11 ±

481   -0.03) compared to of the light ones (light objects = -0.12 ± 0.03; *p = 0.04)* whereas this difference was

482   absent during planning (heavy objects = 0.02 ± 0.04; light objects = -0.04 ± 0.04; *p = 1.00)*. In conclusion,

483   these findings suggest that CSE was not modulated at all for the pSTS and DLPFC groups during lift

484   planning (figure 4). As we have no 'control conditions' (group without virtual lesioning during lift

485   planning), these findings cannot be further interpreted.
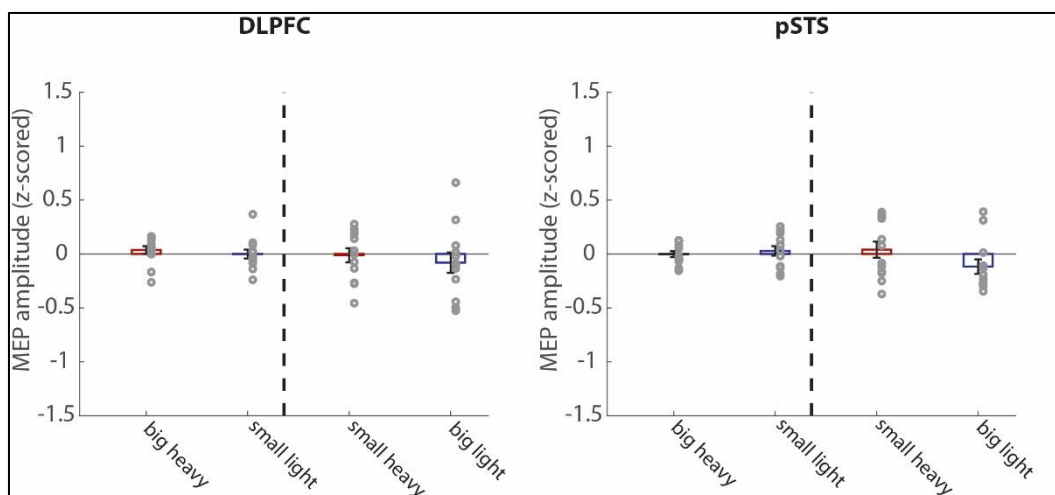
Figure 4. Modulation of corticospinal excitability during lift planning. Average MEP values (z-score) during lift planning pooled across participants for the DLPFC and pSTS groups. Left and right of the dashed line on each figure represent the congruent (big heavy and small light) and incongruent objects (small heavy and big light) respectively. Red and blue indicate heavy and light weights respectively. Each circle (scatter) represents the average MEP value for one participant in that specific condition. All data is presented as the mean ± SEM.

486   To sum up, our results demonstrate that when participants only interact with objects having a

487   congruent size-weight relationship (i.e. big-heavy or small-light), CSE during lift observation is modulated

488   by the object weight as indicated by the size and/or the movement kinematics (control group).

489   Interestingly, when objects with incongruent size-weight relationship (i.e. big light and small heavy) were

490   included (baseline group), weight-driven modulation of CSE was 'suppressed' and CSE was modulated by

491   'object congruency' instead. That is, CSE was facilitated during observed lifting of objects with

492   incongruent properties compared to of objects with congruent properties.

493   Moreover, our results also highlighted that virtual lesioning of pSTS abolishes the suppressive

494   mechanism monitoring the observer's weight expectations and restores weight-driven modulation of

495   CSE during lift observation. As such, our results provide evidence for the causal involvement of pSTS in

496   modulating CSE by monitoring the observer's weight expectations during the observation of hand-object

497   interactions. In addition, virtual lesioning of DLPFC eradicated both the suppressive mechanism as well as

498   weight-driven motor resonance: During lift observation, CSE was not modulated at all. Accordingly, these

499   findings suggest that DLPFC is causally involved in a 'general' modulation of CSE during the observation

500   of hand-object interactions. To end, we did not find significant differences between the DLPFC and pSTS

501   groups for lift planning. Considering that we have no 'control' group to compare with, these findings

502   cannot be further interpreted.

503

504   <u>Force parameters of the participants</u>

505   As mentioned before, we pooled all data with respect to factors related to TMS timing as preliminary

506   analyses revealed that predictive force planning of the participants was not altered by single pulse TMS

507   *Normalized peak grip force rates*. For both the group comparisons on the congruent objects only

508   (all four groups) and on the objects with both congruency types (baseline, DLPFC and pSTS groups)

509   neither the main effect of GROUP nor any of its interactions effects were significant (*all F < 0.86, all p >*

510   *0.47, all η^2_p < 0.04).*

511   First, for only the congruent objects these findings suggest that there is no evidence that the

512   experimental groups scaled their grip forces (i.e. peak GFr values) differently, irrespective of whether

513   they were exposed to only congruent object (control group) or to both congruent and incongruent

514   objects (baseline, DLPFC and pSTS groups). Second, these findings also provide no evidence that virtual

515   lesioning of either DLPFC or pSTS (DLPFC and pSTS groups) affected predictive grip force scaling based on

516   lift observation compared to receiving no virtual lesioning (control and baseline groups). Aside from

517   these results, all groups increased their grip forces significantly faster for the big heavy cube (big heavy =

19

518   0.48 ± 0.03) than for the small light one (small light = -0.43 ± 0.03) *(main effect of CUBE: (F$_{(1,55)}$ = 353.70,*

519   *p < 0.001, η²$_p$ = 0.87).* All group averages are shown on figure 5.
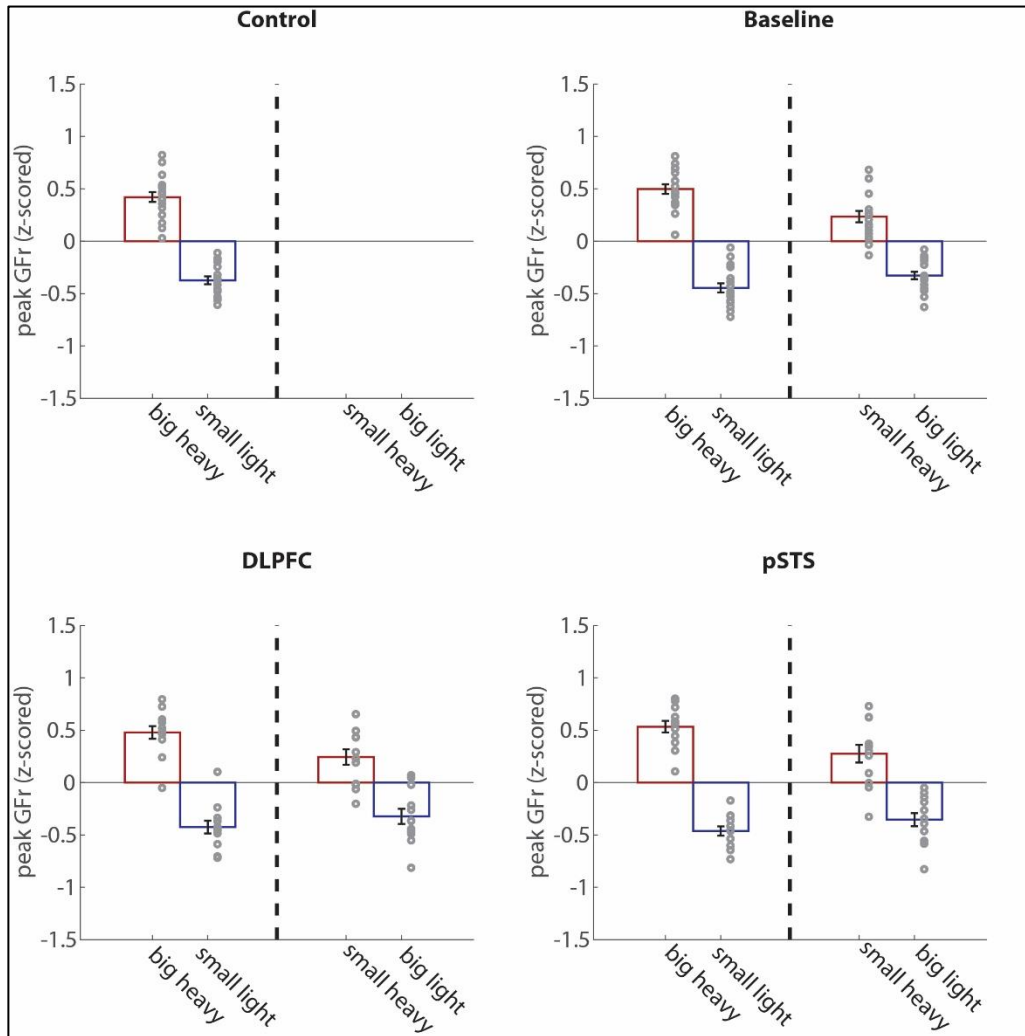
Figure 5. Peak grip force rates of the participants. Average peak grip force rate (GFr) value (z-scored) for each group separately. Left and right of the dashed line on each figure represent the congruent (big heavy and small light) and incongruent objects (small heavy and big light), respectively. Red and blue indicate heavy and light weights, respectively. Each circle (scatter) represents the average peak grip force rate value for one participant in that specific condition. All data is presented as the mean ± SEM. No intra-group significant differences are shown on this figure.

520   Moreover, these findings are similar for the groups that interacted with both congruent and

521   incongruent objects. That is, the baseline, DLPFC and pSTS groups increased their grip forces significantly

522   faster for the heavy objects (heavy = 0.38 ± 0.03) than for the light ones (light = -0.39 ± 0.02; *p < 0.001*)

523   *(main effect of WEIGHT: (F$_{(1,38)}$ = 255.93, p < 0.001, η²$_p$ = 0.87).* However, although these groups were

524   able to scale their grip forces to the actual object weight, they were still biased by the size as they

525   increased their grip forces significantly faster for the big objects (big objects = 0.08 ± 0.02) than for the

526   smaller ones (small objects = -0.10 ± 0.02; *p < 0.001*) *(main effect of SIZE: ($F_{(1,38)}$ = 23.69, p < 0.001, η^2_p =*

527   *0.38).* Lastly, post-hoc analysis of the significant interaction effect WEIGHT X SIZE *($F_{(1,38)}$ = 5.42, p = 0.025,*

528   *η^2_p = 0.12)* highlighted that these groups also increased their grip forces significantly faster for the big

529   heavy object (big heavy = 0.50 ± 0.03) than for the small heavy one (small light = 0.25 ± 0.04; *p < 0.001).*

530   This difference was absent for the light objects *(*small light = -0.44 ± 0.03; big light = -0.34 ± 0.03*; p =*

531   *0.08).*
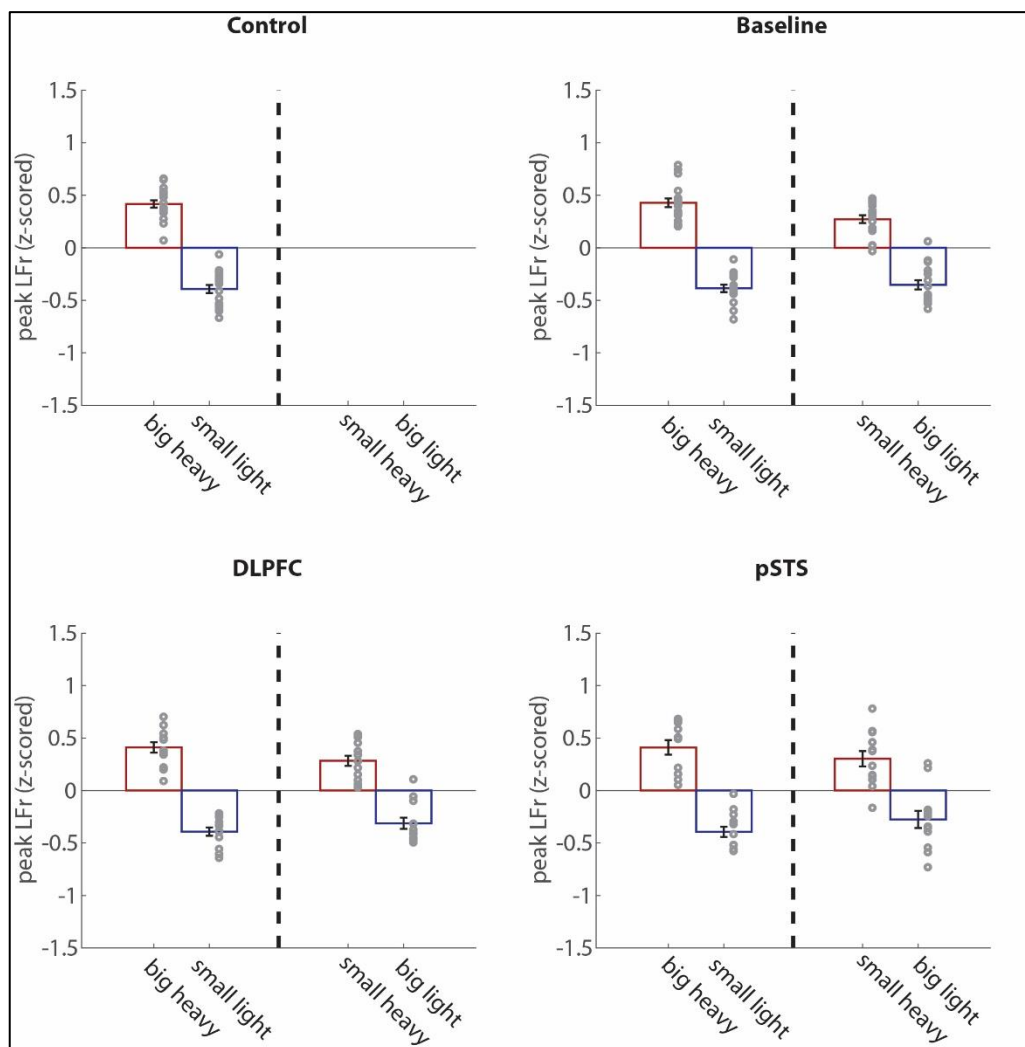
Figure 6. Peak load force rates of the participants. Average peak load force rate (LFr) values (z-scored) for each group separately. Left and right of the dashed line on each figure represent the congruent (big heavy and small light) and incongruent objects (small heavy and big light), respectively. Red and blue indicate heavy and light weights, respectively. Each circle (scatter) represents the average peak load force rate value for one participant in that specific condition. All data is presented as the mean ± SEM. No intra-group significant differences are shown on this figure.

532   *Normalized peak load force rates.* The findings for peak LFr were nearly identical to those for

533   peak GFr. Indeed, for both comparisons [congruent objects only: all groups; both congruent and

534   incongruent objects: baseline, DLPFC and pSTS groups], the main effect of GROUP as well as all its

535   interactions effects were not significant (*all F < 0.72, all p > 0.49, all η^2_p < 0.04*). Accordingly, we did not

536   find any evidence that predictive load force planning based on lift observation was affected by (1) the

537   presence of the incongruent objects (control group vs baseline, DLPFC and pSTS groups) (2) or by the

538   virtual lesioning of DLPFC or pSTS (control and baseline groups vs DLPFC and pSTS groups). Similar to our

539   findings for peak GFr, participants increased their load forces significantly faster for the big heavy cube

540   (big heavy = 0.42 ± 0.02) than for the small light one (small light = -0.39 ± 0.02; *p < 0.001*) (*main effect of*

541   *CUBE: (F$_{(1,55)}$ = 339.57, p < 0.001, η^2_p = 0.86)*.

542   Again, the baseline, DLPFC and pSTS groups, that interacted with both congruent and

543   incongruent objects, increased their load forces significantly faster for the heavy objects (heavy = 0.35 ±

544   0.02) than for the light ones (light = -0.35 ± 0.2; *p < 0.001*) (*main effect of WEIGHT: (F$_{(1,38)}$ = 304.80, p <*

545   *0.001, η^2_p = 0.89)* although they were also biased by object size (big: peak LFr = 0.05 ± 0.02; small: peak

546   LFr = -0.05 ± 0.02; *p = 0.004*) (*main effect of SIZE: (F$_{(1,38)}$ = 9.10, p = 0.005, η^2_p = 0.19)*. All group averages

547   are shown on figure 6 without intra-group significant differences being shown.

548   *Normalized loading phase duration.* Our findings for the participants' loading phase duration

549   were identical to those for peak GFr: For congruent objects only (all groups) and the congruent and

550   incongruent objects combined (baseline, DLPFC and pSTS groups) our analyses did not show significance

551   for the main effect of GROUP as well as its interaction effects (*all F < 2.07, all p > 0.140, all η^2_p < 0.10*),

552   again suggesting that our experimental groups did not differ significantly from each other. Again, the

553   GLM for the congruent objects only showed that the main effect of CUBE was significant *(F$_{(1,55)}$ =*

554   *2717.64, p < 0.001, η^2_p = 0.90)* indicating that all groups lifted the big heavy object (big heavy = 0.83 ±

555   0.02) slower than the small light one (small light = -0.80 ± 0.02; *< 0.001*).

556   In line with our peak GFr findings, the groups (baseline, DLPFC and pSTS), interacting with both

557   congruent and incongruent objects lifted the heavy objects (heavy = 0.91 ± 0.03) significantly slower than

558   the light ones (light = -0.80 ± 0.02; *p < 0.001*) *(main effect of WEIGHT: F$_{(1,38)}$ = 1139.85, p < 0.001, η^2_p =*

559   *0.97)* although they were still biased by the object size as they lifted the big objects faster than the small

560   ones (big = 0.01 ± 0.01; small = 0.09 ± 0.02; *p < 0.001*) *(main effect of SIZE: F$_{(1,38)}$ = 18.43, p < 0.001, η^2_p =*

561   *0.33)*. Finally, post-hoc analysis of the significant interaction effect WEIGHT X SIZE (*F$_{(1,38)}$ = 23.33, p <*

562   *0.001, η^2_p = 0.38)* revealed that all groups lifted the big heavy object (big heavy = 0.82 ± 0.02)

563   significantly faster than the small heavy one (small heavy = 0.99 ± 0.04; *p < 0.001*) although this

564   difference was absent for the light objects (small light = -0.81 ± 0.02; big light = -0.80 ± 0.03; *p = 1.00)*.

565   All group averages are shown on figure 7 without intra-group significant differences being shown.
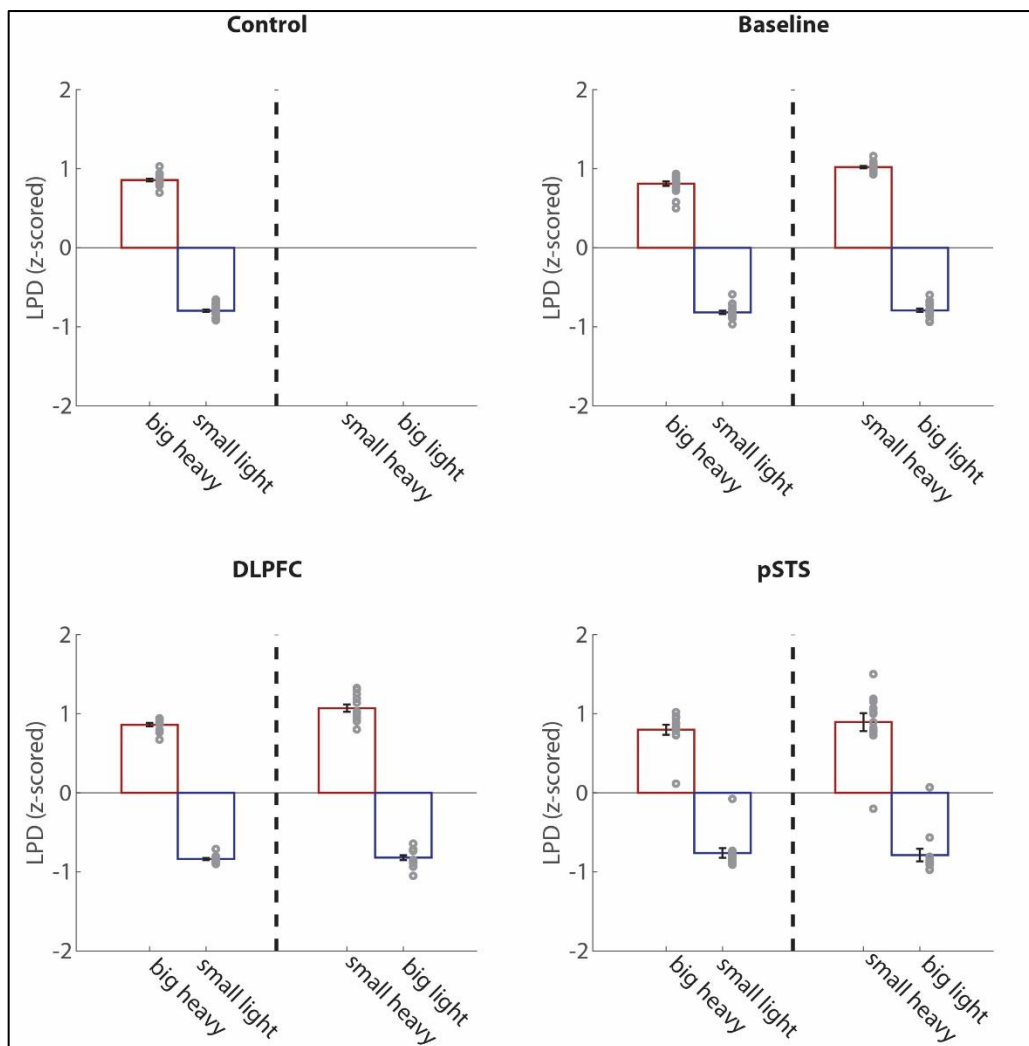
Figure 7. Loading phase duration of the participants. Average loading phase duration (LPD) values (z-scored) for each group separately. Left and right of the dashed line on each figure represent the congruent (big heavy and small light) and incongruent objects (small heavy and big light), respectively. Red and blue indicate heavy and light weights, respectively. Each circle (scatter) represents the average loading phase duration for one participant in that specific condition. All data is presented as the mean ± SEM. No intra-group significant differences are shown on this figure.

566   To sum up, participants lifted the objects [SIZE: big or small by WEIGHT: heavy or light] in turns

567   with the actor and were instructed that the object in their trial was always identical, both in terms of size

568   and weight, to the object the actor lifted in the previous trial. As such, participants could potentially rely

569   on lift observation to estimate object weight and plan their own lifts accordingly. Importantly, our results

570   support this notion: In line with Rens and Davare (2019), our results demonstrate that the groups who

571   interacted with both the congruent and incongruent objects were able to detect the incongruent objects

572   based on observed lifts performed by the actor. Indeed, our findings for the baseline, DLPFC and pSTS

573   groups showed that subjects scaled their fingertip forces to the actual weight of the incongruent objects

574   (main effect of WEIGHT). However, it is important to note that these groups were still biased by object

575   size as, on average, subjects scaled their fingertip forces faster for the large objects than for the small

576   ones (main effect of SIZE). Moreover, exploration of the significant interaction effect of WEIGHT X SIZE

577   for peak GFr and LPD indicated that this effect was primarily driven by the significant difference between

578   heavy objects. Lastly, considering that we did not find significant differences between the baseline group

579   on one side and the DLPFC and pSTS groups on the other side shows that virtual lesioning of either

580   region did not affect predictive lift planning based on lift observation. As such, our findings related to the

581   force parameters indicate that DLPFC and pSTS are not causally involved in neither weight perception

582   during lift observation nor in updating the motor command based on lift observation.

583

584   Force parameters of the actor

585   *Normalized peak grip force rates.* Comparing the congruent objects only across all four groups, the actor

586   increased his grip forces significantly faster for the big heavy object (big heavy = 0.8 ± 0.02) than for the

587   small light one (small light = -0.79 ± 0.01; *p < 0.001*) *(main effect of WEIGHT: $F_{(1,55)}$ = 3328, p < 0.001, η^2_p =*

588   *0.98).* Although the main effect of group was not significant, the interaction effect of GROUP X CUBE

589   *($F_{(3,55)}$ = 5.85, p = 0.002, η^2_p = 0.24)* was. Post-hoc analysis of this interaction effect showed that the actor

590   scaled his grip forces significantly faster for the big heavy object in the baseline group (baseline: big

591   heavy = 0.89 ± 0.03) compared to the control group (control: big heavy = 0.76 ± 0.03, *p = 0.02*). However,

592   all other between-group differences in the actor's lifting performance for the big heavy object were not

593   significant (DLPFC: big heavy = 0.88 ± 0.04; pSTS: big heavy = 0.78 ± 0.03; *all p > 0.12)*. Conversely, this

594   was identical for the small light object with the actor scaling his grip forces significantly slower for the

595   small light object in the baseline group (baseline: small heavy = -0.84 ± 0.02) than in the control group

596   (control: small heavy = -0.72 ± 0.02; *p = 0.05)*. Again, all other between-group actor differences for the

597   small light object were not significant (DLPFC: small light = -0.83 ± 0.03; pSTS: small light = -0.76 ± 0.03;

598   *all p > 0.24)*.

599   For the comparisons including the incongruent objects (baseline, DLPFC and pSTS groups), it is

600   important to note that the interaction effect SIZE X WEIGHT ($F_{(1,38)}$ = 5.52, p = 0.02, η^2_p = 0.13) was

601   significant. Post-hoc analysis showed that the actor increased his grip forces similarly for the light objects

602   (small light = -0.81 ± 0.02; big light = -0.83 ± 0.03; *p = 1.00)* but not for the heavy ones (big heavy = 0.85 ±

603   0.02; small heavy = 0.79 ± 0.04; *p = 0.03)*. As our results indicate that the actor increased his grip forces

604   slower for the small heavy object suggesting that he was biased by the object's size during his own trials.

605   *Normalized peak load force rates.* In line with our findings for grip force rates, the actor

606   increased his load forces significantly faster for the big heavy cuboid (big heavy = 0.80 ± 0.02) than the

607   small light one (small light = -0.72 ± 0.02; *p < 0.001*) (congruent objects only: *main effect of CUBE: $F_{(1,,55)}$ =*

608   *1950.87, p < 0.001, η^2_p = 0.97)*. Importantly, post-hoc exploration of the significant interaction effect

609   GROUP X CUBE *($F_{(3,55)}$ = 3.87, p = 0.01, η^2_p = 0.17)*, did not reveal any relevant significant differences in

610   the actor's performance between groups on the big heavy object (control = 0.71 ± 0.04; baseline = 0.84 ±

611   0.04; DLPFC = 0.85 ± 0.04; pSTS = 0.79 ± 0.04; *all p > 0.18)* or the small light one (control = -0.63 ± 0.03;

612   baseline = -0.76 ± 0.03; DLPFC = -0.76 ± 0.04; pSTS = -0.71 ± 0.04; *all p > 0.18)*.

613   However, the analysis on both the congruent and incongruent objects, showed that the actor

614   scaled his load forces differently based on object size for both the light objects (small light = -0.74 ± 0.02;

615   big light = -0.82 ± 0.03; *p = 0.05)* and the heavy ones (big heavy = 0.83 ± 0.03; small heavy = 0.74 ± 0.04; *p*

616   *= 0.04) (SIZE X WEIGHT: $F_{(1,,38)}$ = 15.40, p < 0.001, η^2_p = 0.29)*. Finally, it is important to note that neither

617   the main effect of GROUP nor its interaction effects were significant *(all F < 1.03, all p > 0.37, all η^2_p <*

618   *0.5)*. As such, we did not find evidence that the actor scaled his load forces differently for the different

619   experimental groups.

620   *Normalized loading phase duration*. Comparing only the congruent objects across all four groups

621   showed that LPD of the actor was significantly longer when lifting the big heavy object (big heavy = 0.76

622   ± 0.02) than the small light one (small light = -0.85 ± 0.02; *p < 0.001)* (congruent objects only: *main effect*

623   *of CUBE: $F_{(1,55)}$ = 2883.95, p < 0.001, η^2_p = 0.98)*. For the comparison on both the congruent and

624   incongruent objects, the interaction effect SIZE X WEIGHT *$F_{(1,38)}$ = 57.40, p < 0.001, η^2_p = 0.60)* was

625   significant. Critically, the post-hoc analysis revealed that the actor lifted the small objects significantly

626   slower than the big ones. That is, the LPD when lifting the big heavy object (big heavy = 0.76 ± 0.02) was

627   significantly shorter than when lifting the small heavy one (small heavy = 0.89 ± 0.03; *p < 0.001)*.

628   Accordingly, this significant difference was also present for the light objects (small light = -0.84 ± 0.02;

629   big light = -0.68 ± 0.02; *p < 0.001)*. Although these findings suggest that the actor's lifting speed was

630   biased by object size, he still lifted the light objects significantly faster than the heavy ones *(SIZE X*

631   *WEIGHT: all p < 0.001)*.

632   In sum, these findings indicate that, in general, the actor scaled his fingertip forces towards the

633   actual object weight for both the congruent and incongruent objects. However, it is important to note

634   that the actor was biased by object size when interacting with the incongruent objects. Across all groups

635   (except the control group which did not interact with the incongruent objects), the actor increased his

636   fingertip forces faster for the big than for the small objects, resulting in a shorter LPD for the larger

637   objects. Presumably, as participants were able to lift the objects (of which they could only predict object

638   weight by relying on the actor's lifting) skilfully, it is plausible that these found differences in the actor's

639   lifting performance drove the participants' ability to estimate object weight during observed lifting.

640   Accordingly, these differences in observed lifting performance should also have driven modulation of

641   CSE. Finally, except for one difference for normalized grip force rates, the actor scaled his fingertip forces

642   similarly across all groups. Importantly, these findings substantiate that our inter-group differences, with

643   respect to CSE modulation, are not driven by differences in the actor's lifting performance between

644   groups but rather by experimental set-up differences [presence of incongruent objects vs. only

645   congruent objects; virtual lesioning of pSTS or DLPFC vs. no virtual lesion].

646

647   **Discussion**

648   In the present study, we investigated how CSE is modulated during observation of lifting actions

649   (i.e. 'motor resonance'). First, results from our control experiment are in line with previous literature

650   (Alaerts et al., 2010b, 2010a; Senot et al., 2011): When participants observed lifts of objects with a

651   congruent only size-weight relationship, CSE was modulated by object weight. However, our results for

652   the baseline group highlight that these typical bottom-up motor resonance effects are easily suppressed

653   when participants cannot predict object weight based on size: When participants observed lifts of

654   objects with congruent and incongruent size-weight relationships, CSE was larger when observing lifts of

655   incongruent objects, regardless of their size and weight. Interestingly, this suggests that typical motor

656   resonance effects were biased by an 'expectation monitoring mechanism'. However, we found these

657   differences at different time points during action observation (figure 3). Arguably, this time difference

658   indicates that the baseline group was able to perceive the small-light object weight *before* lift-off.

659   Presumably, participants estimated object weight based on the actor's reaching phase as Eastough and

660   Edwards (2007) demonstrated that an individual's reaching phase depends on the object's mass.

661   However, we cannot substantiate this theory as we did not record the actor's reaching phase.

662   In a second experiment, we investigated the causal involvement of top-down inputs in mediating

663   this expectation monitoring mechanism by inducing virtual lesions to either pSTS or DLPFC. Strikingly,

664   pSTS virtual lesions abolished the monitoring mechanism and restored weight-driven motor resonance.

665   Importantly, this suggests that pSTS is pivotal in monitoring weight expectations during lift observation.

666   In contrast, DLPFC virtual lesions eradicated any modulation of motor resonance. As such, these findings

667   provide evidence that DLPFC is causally involved in modulating motor resonance in general. Finally,

668   although virtual lesions of either DLPFC or pSTS altered motor resonance, we found no evidence that

669   predictive force scaling, based on observed visuomotor cues, was affected. Specifically, all subject groups

670   in both experiments scaled their fingertip forces appropriately. This suggests that adequate motor

671   planning is not related to the presence of weight-driven motor resonance effects.

672   With respect to our baseline group, it is noteworthy that Alaerts et al. (2010b) showed that,

673   when participants observed lifts of objects with incongruent properties, motor resonance was still driven

674   by weight as cued by the movement kinematics. Our results contrast theirs by showing that CSE was

675   facilitated when observing lifts of incongruent compared to congruent objects. Importantly, our study

676   differs from Alaerts et al. (2010b) on three major points. First, participants in their study did not interact

677   with the objects. Second, their participants were not required to respond to the observed videos

678   (verbally or behaviourally) and third, whereas we used a skewed proportion of congruent and

679   incongruent trials, they used equal proportions.

680   It is unlikely that our findings for the baseline group are entirely driven by the skewed

681   proportion: Pezzetta et al. (2018) demonstrated with electroencephalography (EEG) that when

682   participants observe a larger proportion of erroneous grasping actions, they still elicit the typical activity

683   related to error monitoring as when smaller proportions were used. Thus, it is likely that the 'expectation

684   monitoring mechanism' in our study is driven by the experimental context rather than by the skewed

685   proportion. Moreover, it has been demonstrated that motor resonance during lift observation is not

686   robust and can be altered by semantic object representations (Senot et al., 2011) and observed lifting

687   performance (Buckingham et al., 2014). In our study, participants were required to respond to the visual

688   stimuli by lifting the objects themselves. Arguably, the contextual importance of accurately estimating

689   object weight during lift observation caused the 'expectation monitoring mechanism' to suppress

690   weight-driven motor resonance. As such, our results provide strong evidence that the contextual

691   differences alter modulation of CSE during lift observation.

692   Generally, it has been considered that motor resonance relies on the putative human mirror

693   neuron system (hMNS). First discovered in macaque monkeys (di Pellegrino et al., 1992), mirror neurons

694   are similarly activated when executing or observing the same action and have been argued to underlie

695   action understanding by 'mapping' observed actions onto the cortical representations involved in their

696   execution (Cattaneo and Rizzolatti, 2009). It has been substantiated that the putative hMNS is primarily

697   located in M1, ventral premotor cortex (PMv) and anterior intraparietal area (AIP) (Rizzolatti et al.,

698   2014). Importantly, AIP, PMv and M1 also constitute the cortical grasping network and are pivotal in the

699   planning and execution of grasping actions [for reviews see: Davare et al. (2011) and Gerbella et al.

700   (2017)] which further substantiates the role of the putative hMNS in action understanding. However, our

701   results for the control and baseline groups cannot be unified under the theory that motor resonance

702   represents an automatic mapping of parameters indicating object weight: Whereas our control

703   experiment supports this theory, our baseline group demonstrated that the automatic mapping can be

704   easily suppressed. As such, our findings suggest that different mechanisms are involved in modulating

705   CSE during action observation.

706   In our second experiment, we investigated the origin of the 'expectation monitoring mechanism'

707   and found that disrupting pSTS activity restores weight-driven motor resonance. This suggests that pSTS

708   is causally involved in modulating expectation-driven motor resonance. These findings are plausible as

709   pSTS is crucial in perceiving biological motion (Grossman et al., 2005), which is indicative of object weight

710   (Hamilton et al., 2007), and also in monitoring execution errors during action observation (Pelphrey et

711   al., 2004). Although pSTS does not contain mirror neurons (Hickok, 2009, 2013) and shares no reciprocal

712   connections with M1 (Iacoboni, 2005; Nelissen et al., 2011), it has access to the putative hMNS through

713   reciprocal connections with AIP (Nelissen et al., 2011; Galletti and Fattori, 2017). Plausibly, pSTS

714   modulates CSE through AIP-PMV and PMv-M1 connections (Davare et al., 2011; Nelissen et al., 2011;

715   Gerbella et al., 2017). Indeed, our results suggest that pSTS monitors the weight expectations during

716   observed lifting and masks typical motor resonance effects when expectations can be incorrect.

717   Potentially, virtual lesioning of pSTS abolishes expectation-related input to AIP, restoring the automatic

718   mapping of observed movement parameters. In addition, when expectations are never tested (control

719   group), pSTS might not provide this top-down input and does not mask weight-driven motor resonance.

720   However, future research is necessary to substantiate this theory. Finally, our results also suggest that

721   pSTS does not mediate weight perception as the virtual lesion did not affect predictive lift planning.

722   We also investigated the causal involvement of DLPFC in monitoring weight expectations: Our

723   results suggest that virtual lesioning of DLPFC eradicated not only the expectation monitoring

724   mechanism but also weight-driven motor resonance. As such, our results argue that DLPFC is pivotal in

725   modulating CSE during lift observation, irrespective of the underlying mechanism. Interestingly, our

726   results align with those of Ubaldi et al. (2015): They showed that when motor resonance effects were

727   altered by a visuomotor training task, the trained resonance could be eradicated by virtual lesioning of

728   DLPFC, suggesting that DLPFC is critical in modulating rule-based motor resonance. Importantly, our

729   results extend on theirs by demonstrating that virtual lesioning of DLPFC eradicates not only trained

730   responses but also those which are considered to be automatic. It is plausible that DLPFC can modulate

731   motor resonance: Although it has been considered that DLPFC does not contain mirror neurons (Hickok,

732   2009, 2013), it is reciprocally connected with PMv (Badre and D'Esposito, 2009) and is involved in action

733   observation and processing contextual information (Raos and Savaki, 2017; Rozzi and Fogassi, 2017).

734   Finally, in line with the findings for the pSTS group, virtual lesioning of DLPFC did not affect predictive lift

735   planning.

736   A limitation of the present study is that we only used one TMS timing in the virtual lesion groups,

737   due to time constrains. We only probed motor resonance after observed lift-off as we found the

738   strongest effects of the suppressive mechanisms for our baseline group at this timing. In addition, Ubaldi

739   et al. (2015) demonstrated that motor resonance driven by visuomotor associations is only altered late

740   but not early during movement observation. Therefore, it seemed valid to focus on the late timing. A

741   second limitation concerns the absence of sham cTBS in experiment 2. However, virtual lesioning of

742   DLPFC and pSTS modulated CSE differently indicating that the stimulation site was of importance. Lastly,

743   probing motor resonance when observing lifts of congruent objects only, combined with virtual lesions

744   of DLPFC or pSTS, could further substantiate the findings of the present study.

745   In conclusion, the present study demonstrates that motor resonance effects are not robust but

746   influenced by the cognitive context. We argue that motor resonance should be carefully interpreted in

747   light of the putative hMNS functional roles. Our results indicate that bottom-up motor resonance effects,

748   driven by observed movement parameters, can only be measurable when top-down inputs from pSTS

749   are not triggered by expectation monitoring mechanisms. Moreover, DLPFC is pivotal in the global

750   modulation of CSE during action observation. Altogether, these findings shed new light on the

751   theoretical framework in which motor resonance effects occur and overlap with other cortical processing

752   essential for the sensorimotor control of movements.

753

754   **Bibliography**

755   Alaerts, K.; Senot, P.; Swinnen, S. P.; Craighero, L.; Wenderoth, N.; Fadiga, L. Force Requirements of

756   Observed Object Lifting Are Encoded by the Observer's Motor System: A TMS Study. *Eur. J. Neurosci.*

757   **2010a**, *31* (6), 1144–1153.

758   Alaerts, K.; Swinnen, S. P.; Wenderoth, N. Observing How Others Lift Light or Heavy Objects: Which

759   Visual Cues Mediate the Encoding of Muscular Force in the Primary Motor Cortex? *Neuropsychologia*

760   **2010b**, *48* (7), 2082–2090.

761   Alaerts, K.; de Beukelaar, T. T.; Swinnen, S. P.; Wenderoth, N. Observing How Others Lift Light or Heavy

762   Objects: Time-Dependent Encoding of Grip Force in the Primary Motor Cortex. *Psychol. Res.* **2012**, *76* (4),

763   503–513.

764   Arfeller, C.; Schwarzbach, J.; Ubaldi, S.; Ferrari, P.; Barchiesi, G.; Cattaneo, L. Whole-Brain Haemodynamic

765   After-Effects of 1-Hz Magnetic Stimulation of the Posterior Superior Temporal Cortex During Action

766   Observation. *Brain Topogr.* **2013**, 278–291.

767   Badre, D.; D'Esposito, M. Is the Rostro-Caudal Axis of the Frontal Lobe Hierarchical? *Nat. Rev. Neurosci.*

768   **2009**, *10* (9), 659–669.

769   Baugh, L. a.; Kao, M.; Johansson, R. S.; Flanagan, J. R. Material Evidence: Interaction of Well-Learned

770   Priors and Sensorimotor Memory When Lifting Objects. *J. Neurophysiol.* **2012**, *108*, 1262–1269.

771   Buckingham, G.; Wong, J. D.; Tang, M.; Gribble, P. L.; Goodale, M. A. Observing Object Lifting Errors

772   Modulates Cortico-Spinal Excitability and Improves Object Lifting Performance. *Cortex* **2014**, *50*, 115–

773   124.

774   Castiello, U. The Neuroscience of Grasping. *Nat. Rev. Neurosci.* **2005**, *6* (9), 726–736.

775   Cattaneo, L.; Rizzolatti, G. The Mirror Neuron System. *Arch. Neurol.* **2009**, *66* (5), 557–560.

776   Cattaneo, L.; Sandrini, M.; Schwarzbach, J. State-Dependent TMS Reveals a Hierarchical Representation

777   of Observed Acts in the Temporal , Parietal , and Premotor Cortices. *Cereb. Cortex* **2010**, No. September.

778   Davare, M.; Kraskov, A.; Rothwell, J. C.; Lemon, R. N. Interactions between Areas of the Cortical Grasping

779   Network. *Curr. Opin. Neurobiol.* **2011**, *21* (4), 565–570.

780   Duque, J.; Greenhouse, I.; Labruna, L.; Ivry, Ri. Physiological Markers of Motor Inhibition during Human

781   Behavior. *Trends Neurosci.* **2017**.

782   Eastough, D.; Edwards, M. G. Movement Kinematics in Prehension Are Affected by Grasping Objects of

783   Different Mass. *Exp. Brain Res.* **2007**, *176* (1), 193–198.

784   Fadiga, L.; Fogassi, L.; Pavesi, G.; Rizzolatti, G. Motor Facilitation During Action Observation: A Magnetic

785   Stimulation Study. *J. Neurophysiol.* **1995**, *73* (6), 2608–2611.

786   Galletti, C.; Fattori, P. The Dorsal Visual Stream Revisited: Stable Circuits or Dynamic Pathways? *Cortex*

787   **2017**, 1–15.

788   Gerbella, M.; Rozzi, S.; Rizzolatti, G. The Extended Object-Grasping Network. *Exp. Brain Res.* **2017**, *235*

789   (10), 2903–2916.

790   Gordon; Forssberg; Johansson; Westling. Visual Size Cues in the Programming of Manipulative Forces

791   during Precision Grip. *Exp. Brain Res.* **1991**, *83* (3), 447–482.

792   Grossman, E. D.; Battelli, L.; Pascual-Leone, A. Repetitive TMS over Posterior STS Disrupts Perception of

793   Biological Motion. *Vision Res.* **2005**, *45* (22), 2847–2853.

794   Hamilton, A. F. D. C.; Joyce, D. W.; Flanagan, J. R.; Frith, C. D.; Wolpert, D. M. Kinematic Cues in

795   Perceptual Weight Judgement and Their Origins in Box Lifting. *Psychol. Res.* **2007**, *71* (1), 13–21.

796   Hickok, G. Eight Problems for the Mirror Neuron Theory of Action Understanding in Monkeys and

797   Humans. *J. Cogn. Neurosci.* **2009**, *21* (7), 1229–1243.

798   Hickok, G. Do Mirror Neurons Subserve Action Understanding? *Neurosci. Lett.* **2013**, 6–8.

799   Huang, Y.; Edwards, M. J.; Rounis, E.; Bhatia, K. P.; Rothwell, J. C. Theta Burst Stimulation of the Human

800   Motor Cortex. *Neuron* **2005**, *45*, 201–206.

801   Iacoboni, M. Neural Mechanisms of Imitation. *Curr. Opin. Neurobiol.* **2005**.

802   Johansson, R.; Westling, G. Coordinated Isometric Muscle Commands Adequately and Erroneously

803   Programmed for the Weight during Lifting Task with Precision Grip. *Exp. Brain Res.* **1988a**, *71* (1), 59–71.

804   Johansson, R. S.; Westling, G. Programmed and Triggered Actions to Rapid Load Changes during Precision

805   Grip. *Exp. Brain Res.* **1988b**, *71* (1), 72–86.

806   Jung, N. H.; Delvendahl, I.; Kuhnke, N. G.; Hauschke, D.; Stolle, S.; Mall, V. Navigated Transcranial

807   Magnetic Stimulation Does Not Decrease the Variability of Motor-Evoked Potentials. *Brain Stimul.* **2010**,

808   *3* (2), 87–94.

809   Kilner, J. M. More than One Pathway to Action Understanding. *Trends Cogn. Sci.* **2012**, *15* (8), 352–357.

810   Miller, E. K.; Cohen, J. D. An Integrative Theory of Prefrontal Cortex. **2001**, 167–202.

811   Mylius, V.; Ayache, S. S.; Ahdab, R.; Farhat, W. H.; Zouari, H. G.; Belke, M.; Brugières, P. Definition of

812   DLPFC and M1 According to Anatomical Landmarks for Navigated Brain Stimulation: Inter-Rater

813   Reliability, Accuracy, and Influence of Gender and Age. *Neuroimage* **2013**, *78*, 224–232.

814   Nelissen, K.; Borra, E.; Gerbella, M.; Rozzi, S.; Luppino, G.; Vanduffel, W.; Rizzolatti, G.; Orban, G. A.

815   Action Observation Circuits in the Macaque Monkey Cortex. *J. Neurosci.* **2011**, *31* (10), 3743–3756.

816   Oldfield, R. C. The Assessment and Analysis of Handedness: The Edinburgh Inventory. *Neuropsychologia*.

817   1971, pp 97–113.

818   Pazzaglia, M.; Smania, N.; Corato, E.; Aglioti, S. M.; Psicologia, D.; Sapienza, L.; Lucia, F. S. Neural

819   Underpinnings of Gesture Discrimination in Patients with Limb Apraxia. **2008**, *28* (12), 3030–3041.

820   di Pellegrino, G.; Fadiga, L.; Fogassi, L.; Gallese, V.; Rizzolatti, G. Understanding Motor Events: A

821   Neurophysiological Study. *Exp. Brain Res.* **1992**, *91* (1), 176–180.

822   Pelphrey, K. A.; Morris, J. P.; Mccarthy, G. Grasping the Intentions of Others: The Perceived Intentionality

823   of an Action Influences Activity in the Superior Temporal Sulcus during Social Perception. *J. Cogn.*

824   *Neurosci.* **2004**, 1706–1716.

825   Pezzetta, X. R.; Nicolardi, V.; Tidoni, E.; Aglioti, S. M. Error , Rather than Its Probability , Elicits Specific

826   Electrocortical Signatures : A Combined EEG-Immersive Virtual Reality Study of Action Observation. *J.*

827   *Neurophysiol.* **2018**, 1107–1118.

828   Raos, V.; Savaki, H. E. The Role of the Prefrontal Cortex in Action Perception. *Cereb. Cortex* **2017**, No.

829   October, 4677–4690.

830   Rens, G.; Davare, M. Observation of Both Skilled and Erroneous Object Lifting Can Improve Predictive

831   Force Scaling in the Observer. *Front. Hum. Neurosci.* **2019**, *13* (October), 1–13.

832   Rizzolatti, G.; Cattaneo, L.; Fabbri-destro, M.; Rozzi, S. Cortical Mechanisms Underlying the Organization

833   of Goal-Directed Actions and Mirror Neuron-Based Action Understanding. *Physiol. Rev.* **2014**, 655–706.

834   Rossi, S.; Hallett, M.; Rossini, P. M.; Pascual-leone, A. Screening Questionnaire before TMS: An Update.

835   *Clin. Neurophysiol.* **2011**, *122* (8), 1686.

836   Rozzi, S.; Fogassi, L. Neural Coding for Action Execution and Action Observation in the Prefrontal Cortex

837   and Its Role in the Organization of Socially Driven Behavior. **2017**, *11* (September), 1–9.

838   Senot, P.; D'Ausilio, A.; Franca, M.; Caselli, L.; Craighero, L.; Fadiga, L. Effect of Weight-Related Labels on

839   Corticospinal Excitability during Observation of Grasping: A TMS Study. *Exp. Brain Res.* **2011**, *211* (1),

840   161–167.

841   Tidoni, E.; Borgomaneri, S.; di Pellegrino, G.; Avenanti, A. Action Simulation Plays a Critical Role in

842   Deceptive Action Recognition. *J. Neurosci.* **2013**, *33* (2), 611–623.

843   Ubaldi, S.; Barchiesi, G.; Cattaneo, L. Bottom-up and Top-down Visuomotor Responses to Action

844   Observation. *Cereb. Cortex* **2015**, *25* (4), 1032–1041.

845